A Positive Charge in an Antimalarial Compound Unlocks Broad-spectrum Antibacterial Activity

Maria Braun-Cornejo,[1,2,3] Mitchell Platteschorre,[1] Vincent de Vries,[1] Patricia Bravo,[4,5] Vidhisha Sonawane,[6] Mostafa M. Hamed,[3] Jörg Haupenthal,[3] Norbert Reiling,[6,7] Matthias Rottmann,[4] Dennis Piet,[1] Peter Maas,[1] Eleonora Diamanti,[3] and Anna K. H. Hirsch.[2,3*]

[1] Specs Research Laboratory, Specs Compound Handling, B.V., Bleiswijkseweg 55, 2712 PB Zoetermeer, The Netherlands.

[2] Department of Pharmacy, Saarland University, Campus Building E8.1, 66123 Saarbrücken, Germany.

[3] Helmholtz Institute for Pharmaceutical Research Saarland (HIPS) – Helmholtz Centre for Infection Research (HZI), Campus Building E8.1, 66123 Saarbrücken, Germany.

[4] Swiss Tropical and Public Health Institute Kreuzstrasse 2, 4123 Allschwil, Switzerland.

[5] Universität Basel, Petersplatz 1, 4003 Basel, Switzerland.

[6] Microbial Interface Biology, Research Center Borstel, Leibniz Lung Center, 23845 Borstel, Germany.

[7] German Center for Infection Research (DZIF), Partner Site Hamburg-Lübeck-Borstel-Riems, 23845 Borstel, Germany.

*Corresponding author: Anna.Hirsch@helmholtz-hips.de

Abstract

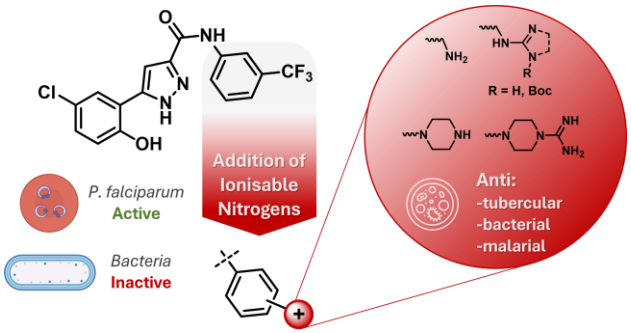

In this study, we synthesised a library of eNTRy-rule-complying compounds by introducing ionisable nitrogens to an antimalarial compound. These positively-charged derivatives gained activity against both Gram-negative and -positive bacteria, *Mycobacterium tuberculosis* and boosted *Plasmodium falciparum* inhibition to the double-digit nanomolar range. Overcoming and remaining inside the cell envelope of Gram-negative bacteria is one of the major difficulties in antibacterial drug development. The eNTRy rules (N = ionisable nitrogen, T = low three-dimensionality, R = rigidity) can be a useful structural guideline to improve accumulation of small molecules in Gram-negative bacteria. With the aim of unlocking Gram-negative activity, we added amines and (cyclic) *N*-alkyl guanidines to an already flat and rigid pyrazole-amide class. To test their performance, we compared these eNTRy-rule-complying compounds to closely related non-complying ones through phenotypic assay screenings of various pathogens (*P. falciparum*, *Escherichia coli, Acinetobacter baumannii*, *Pseudomonas aeruginosa*, *Staphylococcus aureus*, *Streptococcus pneumoniae,* and *M. tuberculosis*) obtaining a handful of broad-spectrum hits. The results support the working hypothesis and even extend its applicability, the studied pyrazole-amide class adheres to the eNTRy rules; non-compliant compounds do not kill any of the bacteria tested, while compliant compounds largely showed inhibition of Gram-negative, -positive, and *M. tuberculosis* bacteria in the single-digit micromolar range.

Keywords: antimicrobial resistance, eNTRy rules, antimalarial, broad-spectrum antibiotic, antitubercular, Gram-negative accumulation.

Introduction

Antimicrobial resistance is increasing rapidly and has become a major global health threat.[1] The World Health Organisation (WHO) highlights the urgency for novel treatments against Gram-negative bacteria

(GNB).[2] Over the past five decades, few new antibiotic classes have been approved, with Gram-negative active ones being vastly underrepresented.[3] Therefore, research and development of antibacterial drug candidates should focus more on targeting GNB, ideally designing novel chemical classes with unprecedented modes of action.[4]

The difficulty of small compounds to permeate and remain inside GNB's cell is the main reason why many antibiotics are active only against Gram-positive bacteria (GPB).[5–7] Many statistical studies to understand the physicochemical properties that promote compound uptake in GNB have been completed since 1968.[8] However, correlation of molecular properties and their bacterial activity give skewed results for two main reasons: (1) limited number of antibiotic compound classes causes lack of structural diversity; (2) in general it is not possible to separate the properties of a molecule that affect its antibacterial activity from the ones that affect its bacterial bioavailability.[9] A fundamentally different approach was taken in 2017 by developing a biological assay that quantifies compound concentration inside *Escherichia coli* cells, effectively measuring compound bioavailability.[10] Applying this assay to a diverse set of nearly 200 compounds and using computational methods to analyse the results, the Hergenrother group developed the so-called "eNTRy rules" (N = ionisable nitrogen, T = low three-dimensionality, R = rigidity).[10,11] According to these guidelines, compounds containing an ionisable nitrogen, with low globularity and high rigidity are more likely to accumulate inside *E. coli* cells. The group's initial work identified primary amines as the most effective ionisable nitrogen-containing functional group, outperforming secondary and tertiary amines. Since these rules were introduced, many successes of their application to Gram-positive-only starting points to achieve GNB inhibition have been published.[12–15] The most advanced compounds show *in vivo* efficacy, and inhibition of critical GNB pathogens like *Klebsiella pneumoniae* and *Acinetobacter baumannii*, indicating that eNTRy rules have a promising broad applicability.[16–18] In 2021, Hergenrother's team broadened their investigation to other functional groups and revealed that *N*-alkyl guanidiniums perform similarly to primary amines, regarding enhanced accumulation in *E. coli*.[19] This finding aligns with previous work of Masci *et al.*, who observed that the inclusion of an amine or guanidine, into their new antibiotic class was essential to overcome the GNB outer membrane, obtaining enhanced activity against *E. coli*, K. *pneumoniae* and *A. baumannii*.[20] Given that GNB's membrane composition differs between species and individual strains, with *E. coli's* membrane generally being easier to cross, applying the eNTRy rules to other Gram-negative species needs caution.[21–23] For instance, Andrews *et al.* enhanced the polarity of a hit compound to overcome efflux problems in *E. coli* by introducing various ionisable groups, achieving a significant improvement with primary amine derivatives.[24] However, this approach did not translate to *A. baumannii* or *Pseudomonas aeruginosa*. Recently, an extensive investigation across different strains of *E. coli*, *A. baumannii*, and *P. aeruginosa* using a carefully designed library of 80 oxazolidinones, revealed that small structural changes can heavily influence the accumulation and efflux of this class in different GNB.[25] This study suggests that *E. coli* and *A. baumannii* have a more comparable membrane composition than *P. aeruginosa*, which generally proved to be more difficult to target.

These important findings on structural features and properties of small molecules and their relationship with GNB uptake, mark a crucial starting point for the rational design of anti Gram-negative antibiotics. The relevance of these rules for compounds that do not show previous antibiotic activity needs to be assessed, as it would be especially useful and important for accessing novel antibacterial classes and thereby delay the emergence of cross-resistance.[3] Recently, we filtered a screening library for an *in silico* hit-identification study according to the eNTRy guidelines with the aim of increasing *E. coli*

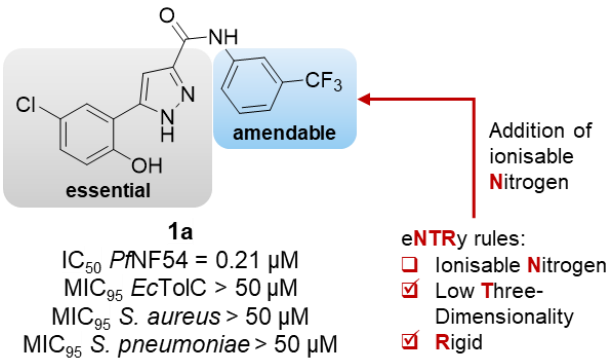

Figure 1: Illustration of our design strategy: use of compound **1a** as antimalarial starting point to incorporate ionisable nitrogen functionalities.

bioavailability.[26] This approach led to the identification of several *E. coli* inhibitors indicating that eNTRy rules are beneficial for the selection of antibacterial compound libraries. Optimisation of the hits, however, demonstrated the challenges of balancing antibacterial activity with target engagement whilst minimising toxicity. In a previous study, we introduced primary amine moieties through amino acid based residues to an antimalarial chemical class, obtaining compounds compliant with the eNTRy rules.[27] These derivatives, however, did not show significant efficacy against *E. coli*, showcasing that the addition of an ionisable nitrogen is not always enough to gain GNB uptake.

In this study, we further investigate the applicability of Hergenrother's guidelines to antimalarial compounds to expand their anti-infective scope. We achieved this by introducing a variety of ionisable nitrogen functionalities to a flat and rigid antimalarial structure (Figure 1). The functional groups comprise various amine motifs, and *N*-alkyl guanidines including novel cyclised forms not previously explored in this context. A concise synthesis yielded 48 derivatives, including neutral controls. The compounds with ionisable nitrogen atoms display broad-spectrum activity against a wide variety of pathogens. In addition to boosting activity against the parasite *Plasmodium falciparum*, many compounds demonstrate antibacterial activity against *E. coli, A. baumannii*, *P. aeruginosa*, *Staphylococcus aureus*, *Streptococcus pneumoniae*, and *Mycobacterium tuberculosis*.

Results and Discussion

Molecular Design. Our antimalarial starting point **1a** originates from previous unpublished work, its structure comprises three aromatic ring systems: a phenol directly connected to a pyrazole with an amide linking to a trifluoromethyl-substituted phenyl ring (Figure 1). The analysis of our hit molecule with the eNTRy rules revealed that it already complies with two out of the three structural properties from Hergenrother's findings. Specifically, it is rigid (less than five rotatable bonds), and the scaffold of three

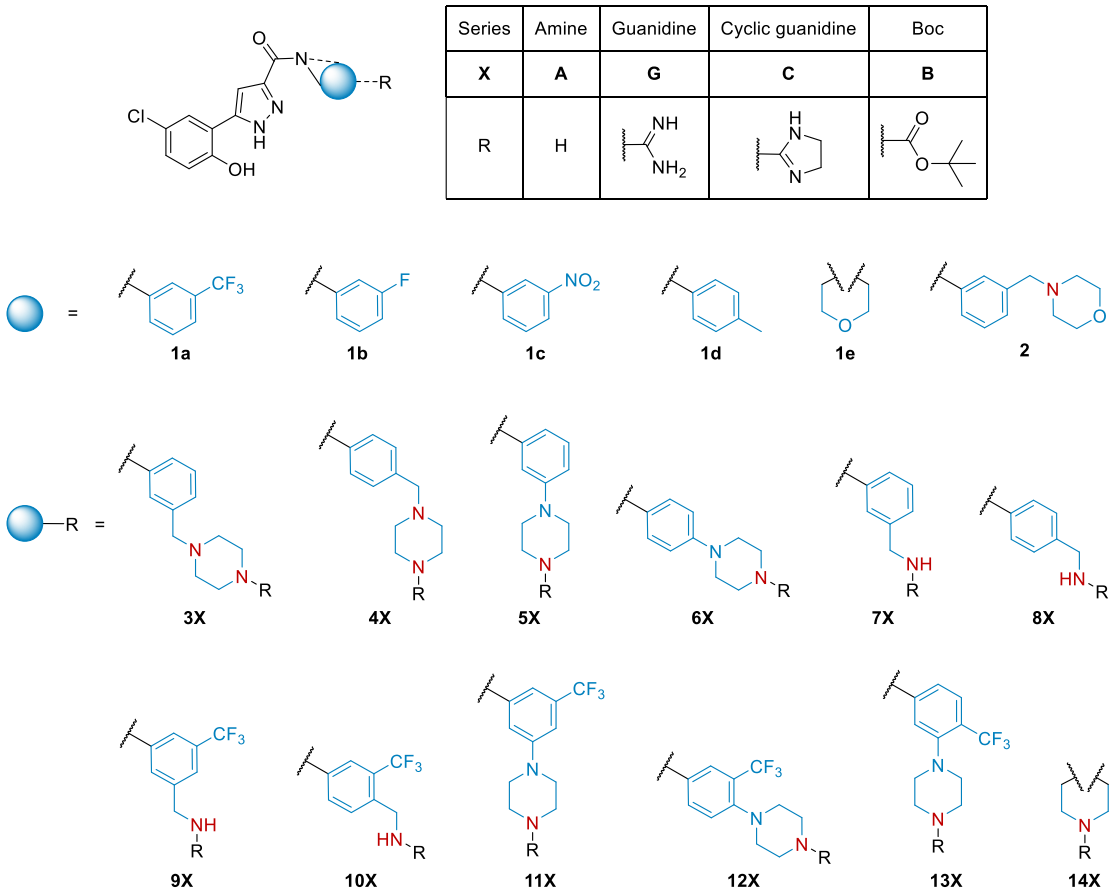

Figure 2: Focused library of pyrazole-amide class, including control compounds (**1a–e** and **3–14B**), amine (**2**, **3–14A**), Guanidine (**5–14G**), and Cyclic-guanidine (**7–11C**) derivatives. Potential ionisable nitrogens in red.

connected aromatic rings is extremely flat (low globularity), but it does not contain an ionisable nitrogen.[10,11] Compound **1a** presents antimalarial activity by inhibiting *P. falciparum* in the moderate nanomolar range but shows no antibacterial activity. Previous work suggests that the phenol and pyrazole moieties are crucial for antimalarial efficacy, whereas the amide-linked phenyl is amenable to changes. Modifications on this part of the molecule are easily accessible synthetically via amide couplings. Therefore, we rationally designed a focused library (Figure 2) of 32 compounds containing ionisable nitrogen atoms while preserving the essential phenol and pyrazole moieties, with the aim of obtaining anti-Gram-negative activity. The introduced positively charged nitrogen-containing functional groups are amines (**A**-series), and *N*-alkyl guanidines (**G**-series). More specifically, amine moieties include methylamines, piperazines, and morpholine. We derived the guanidines from the primary and secondary amines for a direct comparison of the anti-infective profile, with some analogues featuring cyclised guanidines (**C**-series) for added lipophilicity (Figure 2). Additionally, to gain further insights, we included *N*-Boc (**B**-series) protected analogues of the amines as uncharged controls. As additional controls, we also included some alternative electron-withdrawing substituents to the trifluoromethyl of **1a**, namely fluorine **1b** and nitro **1c**. To assess the influence of an electron-donating substituent, we included methyl-derivative **1d** and to evaluate the influence of the aromatic ring we removed it in structures **1e** and **14**.

Synthesis. We optimised the synthesis of the designed library using key chromene amide intermediates **34**–**51**. Initially, we investigated amide couplings of pyrazole-carboxylic acid derivatives with anilines. This procedure was hampered by low yields, and purification and isolation of the products proved difficult. Alternatively, we used commercially available 6-chlorochromene-2-carboxylic acid (**15**) for the amide coupling. Subsequent reaction with hydrazine hydrate formed pyrazole-amide products **1a**–**e**, **2** and **3**–**14B** in quantitative yield (Scheme 1). The amines **16** –**33** used in the amide coupling were largely commercially available, however, maintaining the trifluoromethyl substituent of parent compound **1a** in addition to the ionisable nitrogen functionality, required synthesis of **16**–**20** (Scheme 2).

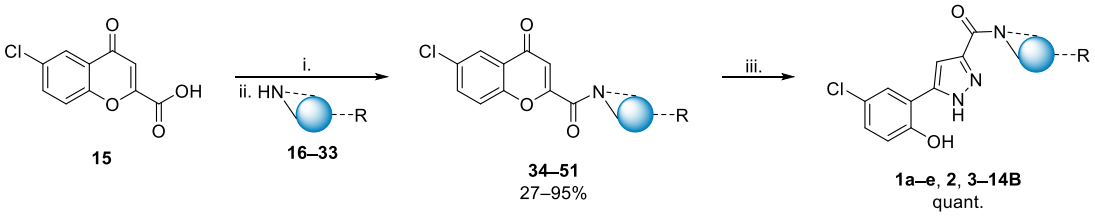

Scheme 1: General synthetic scheme of pyrazole-amides compounds **1a**–**e**, **2** and **3**–**14B**, r*eagents and conditions:* i) DIPEA, HATU, DMF, 0 °C, 30 min; ii.) r.t., 2–24 h;[28] iii.) hydrazine hydrate, EtOH, reflux, 2–18 h.[29]

To minimise the formation of by-products in the amide coupling, the methylamine- and piperazine-substituted anilines needed *N*-Boc protection, which, at the same time allowed to obtain the **B**-series (**3**–**14B**) as control compounds. To obtain aniline **16** and **17**, we selectively *N*-Boc protected methylamine analogues **54** and **55**. Analogue **54** was prepared by reducing the nitro and nitrile groups of **52**, and **55** was commercially available (Scheme 2A). We obtained piperazine-substituted anilines **18** and **19** in a two step synthesis starting with fluorine displacement of derivatives **56** and **57** using 1-Boc piperazine. Subsequent reduction of the nitro group using sodium dithionite gave anilines **18** and **19** in good to moderate yields. The synthesis of aniline **20** required an additional step, because the direct fluorine displacement of **60** using 1-Boc piperazine was unsuccessful. Using an excess of unsubstituted piperazine, however, followed by *N*-Boc protection afforded **62** in a good yield. Lastly, reduction of the nitro group afforded aniline **20** in a modest yield (Scheme 2B).

The obtained compounds of the Boc-series (**3**–**14B**) served as intermediates providing the desired amine series as TFA salts in excellent yields (**3**–**14A**). Following a similar approach, the **A**-series was used to obtain both guanidine series **C** and **G**. The initial guanidinylation strategy for the five-membered ring guanidine series **C** yielded undesired double-guanylated products. Controlling the reaction rate for selective guanidinylation using reagent **63** proved challenging, leading to difficult purifications and

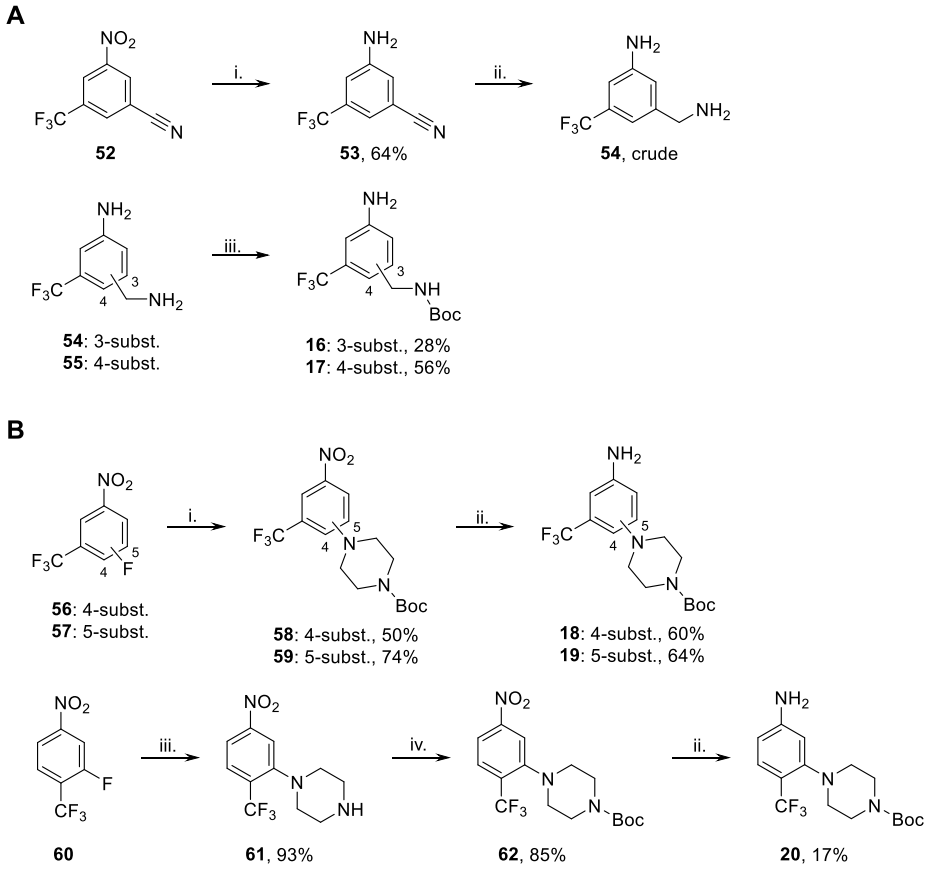

Scheme 2. Synthesis of anilines **16**–**20.** A) Methylamine-substituted anilines, *reagents and conditions:* i) Fe, NH_4Cl, EtOH:H_2O (2:1), reflux, 24 h; ii.) $LiAlH_4$, THF, reflux, 4 h; iii.) Boc_2O, NEt_3, DCM, 0 °C–r.t., 6–24 h.[30] B) Piperazine-substituted anilines, *reagents and conditions:* i.) 1-Boc piperazine, K_2CO_3, DMSO, 100 °C, 18–20 h;[31] ii.) $Na_2S_2O_4$, EtOH, reflux, 6 h; iii.) piperazine, K_2CO_3, 100 °C, DMSO, 24 h;[31] iv.) Boc_2O, DMAP, DCM, r.t., 72 h.[32]

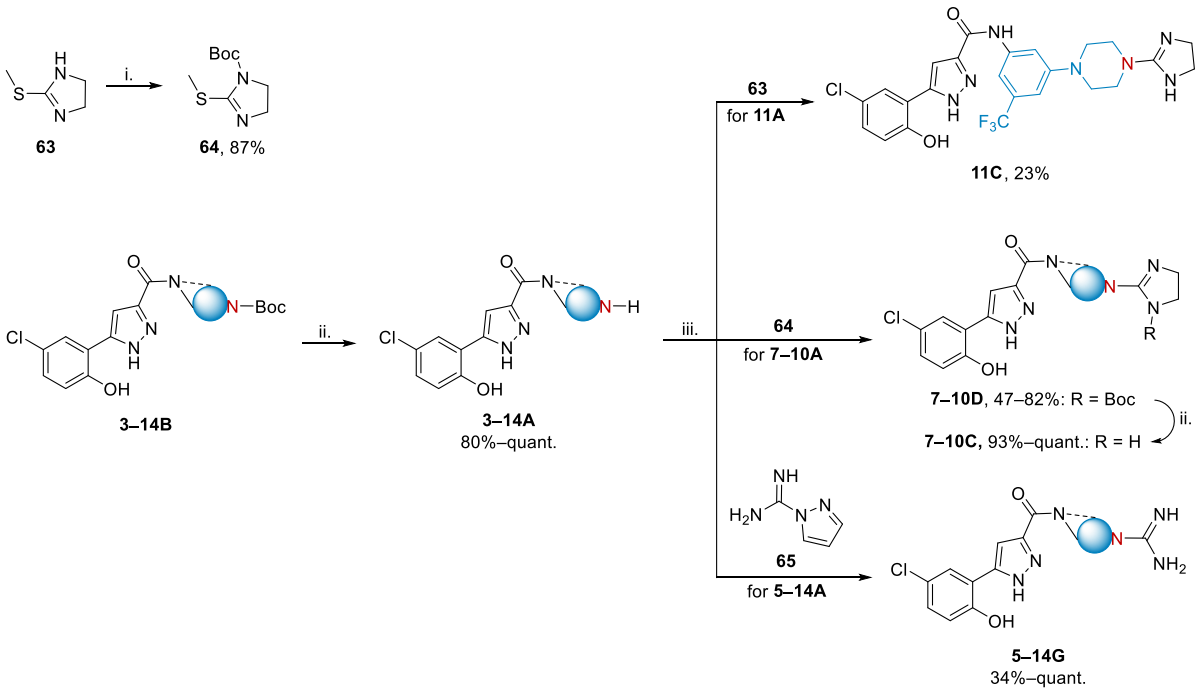

Scheme 3. General synthetic scheme of pyrazole-amides containing ionisable nitrogens: amine (**A**), guanidine (**G**), cyclic-guanidine (**C**) and *N*-Boc cyclic-guanidine (**D**). *Reagents and conditions:* i.) Boc_2O, NEt_3, DCM, r.t., 24 h;[30] ii.) TFA, DCM, r.t., o.n.;[33] iii.) DIPEA, DMF, r.t., o.n.[34–36]

low yield of product **11C** (Scheme 3). To address this issue, we *N*-Boc protected **63**, obtaining the alternative guanidinylation agent **64**. This modification facilitated the synthesis of the remaining cyclic guanidines (**5**–**10C**) *via* their corresponding Boc analogues (**7**–**10D**) in good yields. As piperazines are more lipophilic than methylamines, we opted to exclude piperazine derivatives from the **C** and **D**-series. The *N*-alkyl guanidine series **G** was accessed by employing guanidinylation agent **65**, resulting in moderate to excellent yields (Scheme 3).

Overview of anti-infective activity. We assessed the anti-infective profile of our newly synthesised library against the parasite *P. falciparum,* and various bacterial strains both Gram-negative, and -positive, as well as *M. tuberculosis*. The vast majority of compounds largely retained antimalarial activity (strain *Pf*NF54) compared to the parent compound **1a**, indicating that anti-infective properties were not affected by the addition of a positive charge (Table 1). This finding gave a good foundation to determine antibacterial efficacy of the library and evaluate the applicability of the eNTRy rules. In the case of Gram-negative bacteria, firstly we tested all compounds against the efflux-pump deficient *E. coli* strain *Ec*Δ*tolC*. As the majority of positively charged compounds showed at least moderate *Ec*Δ*tolC* inhibition, we extended the panel and included the *E. coli* wild type *Ec*K12, *A. baumannii* and *P. aeruginosa* strain PA14. Approximately half of the compounds are active against *Ec*K12, however, with significant loss in potency compared to *Ec*Δ*tolC*, indicating efflux liabilities. Many of the *E. coli* inhibitors were also active against *A. baumannii* and PA14. Interestingly, the addition of ionisable nitrogens to this class also yielded excellent activities against *M. tuberculosis* strain *Mtb*H37Rv and GPB. None of our neutral control compounds presented antibacterial activity. These findings confirm that the eNTRy rules are applicable to our pyrazole-amide class. In addition to gaining activity against GNB by introducing ionisable nitrogens, for the first time, we showed that this effect can expand to GPB and *M. tuberculosis*. Excitingly, this approach yielded a new broad-spectrum anti-infective class, with many compounds being active across species. We illustrated the big overlap of active compounds across *Pf*NF54, *Ec*Δ*tolC*, *Mtb*H37Rv and GPB (*S. pneumoniae* or *S. aureus*) in a Venn diagram (Figure 3). In addition, two examples (**7D**, **10G**) inhibit all eight tested pathogens, and an additional eleven compounds (**3G**, **5A**, **6G**, **9**–**11C**, **9G**, **10**–**11A**, **11G**, **13G**) inhibit all pathogens except for *P. aeruginosa,* which is known to be particularly challenging pathogen (Table 1).

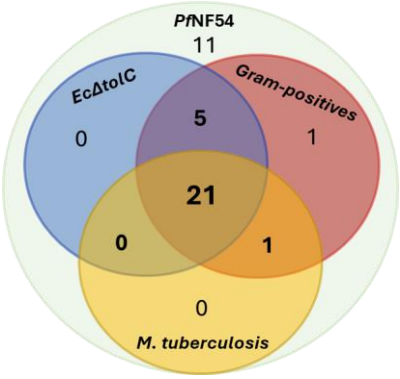

Figure 3: Venn diagram of the active compounds in *Pf*NF54, *Ec*Δ*tolC,* Gram-positive bacteria and M. tuberculosis, indicating the broad-spectrum anti-infective nature of our pyrazole-amide class.

Structure–activity relationships. Our library was designed to investigate various functional groups, mostly containing nitrogens, and their effect on anti-infective properties. In total, we synthesised 48 compounds, 28 of which contain ionisable nitrogen atoms, consisting of thirteen amines (**2**, **3**–**14A**), ten *N*-alkyl guanidines (**5**–**14G**), and five cyclic guanidines (**7**–**11C**). In addition, we tested four Boc protected analogues (**7**–**10D**) of the cyclic guanidines (**7**–**10C**), these functionalities are likely not ionisable in physiological conditions based on computational evaluation (pK_a: ~5.1). The Boc protected analogues (**3**–**14B**) of the amines (**3**–**14A**) serve as more reliable neutral control compounds, as well as compounds **1a**–**d**, which lack ionisable nitrogen atoms altogether. Besides the nature of the functional groups, the main differences between these compounds are the motifs that contain said groups, consisting of piperazines, methylamines, and morpholine. Additionally, the substitution pattern of the motifs changes, with some examples (**9**–**13**) including the trifluoromethyl substituent present in parent compound **1a**.

P. falciparum. Our antimalarial starting point **1a** has an inhibitory concentration in the submicromolar range (*Pf*NF54 IC_{50} = 0.21 μM) which was largely retained in the dedicated library (Table 1). Fourteen compounds (**5**–**6A**, **9**–**13A**, **9**–**11B**, **9**–**10D**, **9G**, **12G**) showed an increase in activity against *Pf*NF54, all of them except for **5A** and **6A** retain the meta-CF_3 substitution on the aromatic ring of **1a**. The two most active

Table 1. Biological activity of pyrazole-amide class in *Plasmodium falciparum* (*Pf*NF54), *Escherichia coli* (*EcΔtolC* and *EcK*12), *Acinetobacter baumannii (Ab), Pseudomonas aeruginosa* (PA14), *Streptococcus pneumoniae* (*Sp*), *Staphylococcus aureus (Sa), Mycobacterium tuberculosis (Mtb*H37Rv), and human liver cells (HepG2).

		Gram-negative				Gram-positive			
Cmp	***Pf*NF54 IC_{50}**	***EcΔtolC* MIC_{95}**	***Ec*K12 inh. at 50 µM**	***Ab* inh. at 50 µM**	**PA14 inh. at 50 µM**	***Sp* MIC_{95}**	***Sa* MIC_{95}**	***Mtb*H37Rv MIC_{90}**	**HepG2 CC_{50}**
1a	0.21	>50	<10%	<10%	<10%	>50	>50	n.d.	>50
1b	0.7	>50	n.d.	n.d.	n.d.	>50	>50	n.d.	n.d.
1c	0.51	>50	n.d.	n.d.	n.d.	>50	>50	>32[a]	n.d.
1d	2.40	>50	n.d.	n.d.	n.d.	>50	>50	n.d.	>50
1e	>5	>50	n.d.	n.d.	n.d.	>50	>50	>16	>50
2	1.1	>50	n.d.	n.d.	n.d.	>50	>50	>16[a]	~50
3A	0.62	45	28%	21%	50%	40	>50	>64	12
3B	1.0	>50	n.d.	n.d.	n.d.	>50	>50	n.d.	25
4A	0.27	40	34%	24%	62%	40	>50	64	13
4B	0.2	>50	n.d.	n.d.	n.d.	>50	>50	n.d.	7
5A	0.13	21	83%	34%	60%	26	37	64	9
5B	0.9	>50	n.d.	n.d.	n.d.	>50	>50	n.d.	>50
5G	0.93	11	32%	<10%	31%	48	23.1	64	>50
6A	0.14	22.5	49%	37%	63%	45	>50	>16[a]	11.8
6B	1.61	>50	n.d.	n.d.	n.d.	>50	>50	n.d.	>50
6G	0.44	9	45%	32%	55%	25	26	64	>50
7A	0.30	47	27%	15%	44%	43	>50	>64	28.4
7B	1.1	>50	n.d.	n.d.	n.d.	>50	>50	n.d.	>50
7C	0.39	13	29%	33%	41%	48.2	22.3	32	>50
7D	0.36	14	56%	77%	55%	31	24.0	64	19
7G	0.21	13	61%	24%	56%	49.0	22	64	>50
8A	1.8	>50	n.d.	n.d.	n.d.	>50	>50	>16[a]	30
8B	1.7	>50	n.d.	n.d.	n.d.	>50	>50	n.d.	>50
8C	0.67	21.5	<10%	12%	10%	>50	49	>64	>50
8D	>5	>50	n.d.	n.d.	n.d.	>50	>50	>64	>50
8G	0.42	47.5	29%	19.9%	41%	>50	22	>64	>50
9A	0.082	8	<10%	MIC_{95} = 49	<10%	11	12.1	32	7
9B	0.2033	>50	n.d.	n.d.	n.d.	30	>50	>64	5.0
9C	0.517	7	<10%	47%	18%	15	9	16	>50
9D	0.15	24.0	<10%	82%	21%	21	12	16	14
9G	0.078	5	MIC_{95} = 46	59%	50%	>50	8	32	>50
10A	0.15	22.9	61%	86%	<10%	23	29	64	13
10B	0.19	>50	n.d.	n.d.	n.d.	>50	>50	n.d.	>50
10C	0.404	5.5	77%	47%	29%	14	8	16	>50
10D	0.14	18	17%	<10%	<10%	>50	11.6	16	11
10G	0.25	3.5	86%	49%	55%	16	5	8	>50
11A	0.05	7	72%	MIC_{95} = 22	<10%	5	6	32	9
11B	0.13	>50	n.d.	n.d.	n.d.	>50	>50	n.d.	4.0
11C	0.59	7	63%	53%	<10%	7	8	8	>50
11G	0.5	4	MIC_{95} = 48	MIC_{95} = 17	25%	28	3.2	8	>25
12A	0.06	18.9	12%	29%	<10%	8	14	16	6
12B	0.56	>50	n.d.	n.d.	n.d.	>50	>50	n.d.	>50
12G	0.2	2.8	51%	33%	<10%	31	2.4	4	30
13A	0.160	>50	n.d.	n.d.	n.d.	29	>50	32	8
13B	0.3418	>50	n.d.	n.d.	n.d.	>50	>50	n.d.	2.8
13G	0.5	5	59%	46%	17%	16	2.5	8	>25
14A	3.3	>50	n.d.	n.d.	n.d.	>50	>50	>16	>50
14G	>5	>50	n.d.	n.d.	n.d.	>50	>50	>64	>50

[a] Not active at maximum solubility; n.d.: not determined. IC_{50}, MIC, and CC_{50} values are in µM.

compounds **11A** and **12A** (IC_{50} ≤ 0.06 μM) contain a piperazine substituent, respectively on meta and *para* positions. In contrast, the compounds without an aromatic ring linked to the nitrogen of the amide (**1e**, **14A**, **14G**) are inactive, suggesting that the aromatic moiety is essential. When it comes to the aromatic ring, para-methylene substitution seems detrimental, methyl derivative **1d**, methylamine **8A** and Boc-protected cyclic guanidine **8D** have a tenfold decrease in activity compared to **1a** (IC_{50} > 2 μM). Similarly, Boc-protected amine derivatives without an additional CF_3 substituent suffer from a significant loss in activity (**5**–**8B**: IC_{50} = 0.9–1.7 μM). Exchanging the trifluoromethyl substituent of **1a** with other electron-withdrawing groups led to a loss in activity (**1b**–**c**: IC_{50} = 0.5–0.7 μM). These findings reveal that the combination of trifluoromethyl substitution and ionisable nitrogen atom can be highly favourable for activity in *Pf*NF54 and that bigger substituents such as piperazine and *N*-Boc piperazine are well-tolerated.

Gram-negative bacteria. The *E. coli* inhibition of all 48 compounds was investigated using the efflux-pump deficient *Ec*Δ*tolC* strain. We obtained 26 hits with a wide range of activities (MIC_{95}: 2.8–47.5 μM, Table 1). None of the neutral control compounds significantly affected the growth of *Ec*Δ*tolC* (Table S1), indicating that these structures were not permeable and that a positive charge is essential for *E. coli* activity. The eleven most potent hits have a single-digit micromolar minimum inhibitory concentration (MIC) and consist of nine (cyclic) guanidines (**6G**, **9**–**13G**, **9**–**11C**,) and two amine derivatives (**9A**,**11A**). Similarly to *Pf*NF54, only one of the top hits does not contain a *m*-CF_3 substituent (**6G**). In addition, the compounds with no antimalarial activity also lack activity against *E. coli*. Only two positively charged antimalarial hits are inactive against *Ec*Δ*tolC* (**2**, **13A**). These findings suggests that the engagement with the anti-infective target is largely consistent across these two species. In the case of *Ec*Δ*tolC* inhibition there is a clear trend indicating that guanidine-type groups enhance potency. When comparing the different positively charged groups of identical scaffolds, the amine derivatives (**A**-series) have the lowest potencies, with one exception (MIC_{95}: **9A** = 8 μM *vs* **9D** = 24 μM). Within the various types of guanidine functionalities (**C**-, **D**-, **G**-series), the *N*-Boc protected cyclic guanidine derivatives (**D**-series) are less active, with the most significant difference observed for scaffold **10** (MIC_{95}: **10D** = 18 μM *vs* **10C** = 5.5 μM *vs* **10G** = 3.5 μM).

To further investigate the antibacterial profile and assess the eNTRy rules' applicability, the 26 *Ec*Δ*tolC* hits (MIC_{95} < 50 μM) were tested against the *E. coli* wild type K12, *A. baumannii* and *P. aeruginosa*. As expected these pathogenic strains were harder to target, nevertheless, fifteen hits (**5**–**6A**, **10**–**11A, 6G**, **7G, 9**–**11G, 13G**, **7D**, **9D**, **9**–**11C**) were identified with moderate inhibition (≥ 45%) at 50 μM compound concentration against *Ec*K12. Structurally, we confirm once again that the guanidine functionality is beneficial for *E. coli* activity, with the two most active compounds being **9G** and **11G**, These structures have *Ec*K12 MIC_{95} values just below 50 μM (**9G** = 46 μM; **11G** = 48 μM), which indicates a tenfold decrease in activity compared to *Ec*Δ*tolC* (**9G** = 5 μM; **11G** = 4 μM), making efflux a main concern for the activity of this class. Noteworthy, the most significant loss of activity is observed for methylamine **9A**, one of the top *Ec*Δ*tolC* inhibitors that did not show any effect on *Ec*K12 growth (**9A** Δ*tolC* MIC_{95} = 8 μM *vs* **9A** K12 < 10% inh. at 50 μM). A similar trend also applies to compound **9D** where the good activity against *Ec*Δ*tolC* did not translate to *Ec*K12 (**9D** Δ*tolC* MIC_{95} = 24 μM *vs* **9D** K12 < 10% inh. at 50 μM). These findings led us to speculate that the structural makeup of compounds **9** seems to be especially prone to *tolC* efflux. In the case of *A. baumannii*, eleven compounds (**7D**, **9D**, **9**–**11C**, **9**–**11G, 13G**, **10**–**11A**) showed a moderate (≥ 45% inh. at 50 μM) to good (MIC_{95} < 25 μM) activity, with **11A** and **11G** as the best hits having an MIC_{95} of 22 μM and 17 μM, respectively. Interestingly, these doubly *meta*-substituted structures are also among the best *E. coli* hits. The remaining nine *A. baumannii* inhibitors also largely contain a CF_3 substituent and (cyclic) guanidines, with all of them except for **9D** being active against *Ec*K12. This big overlap in their inhibitory profile suggest that the bioavailability and target engagement of our pyrazole-amide class is similar in *A. baumannii* and *Ec*K12. When comparing to *P. aeruginosa*, however, the species have less hits in common as illustrated in the Venn diagram (Figure 4). We identified nine compounds (**3**–**6A**, **6**–**7G**, **9**–**10G,7D**) with a moderate effect (≥ 45% inh. at 50 μM) on the growth of *P. aeruginosa* strain PA14. Three of the PA14 hits (**7D**, **9**–**10G**) are also active against the other two GNB wild-types *Ec*K12 and *A. baumannii,* and an additional four compounds

(**5**–**6A**, **6**–**7G**,) share activity with *Ec*K12 (Figure 4). Methylamine derived guanidines seem to be a privileged scaffold for targeting GNB, they appear in the three common hits across all tested GNB and in several other shared hit scaffolds of *E. coli* and *A. baumannii* (**9**–**10C**) or PA14 (**3G**). Overall, the potencies of the PA14 hits are the lowest we obtained across all pathogens (Table 1). The CF_3 substituent and the guanidine moieties seem to be significantly less effective in targeting PA14 compared to the other GNB. In contrast, amines with (methyl-) piperazine motifs yielded better results. These findings align with the structure–uptake study on Oxazolidinones where they identified a CF_3-substituted phenyl motif as a liability to *P. aeruginosa* outer membrane permeation and also concluded that *P. aeruginosa* is more divergent compared to *E. coli* and *A. baumannii*.[25]

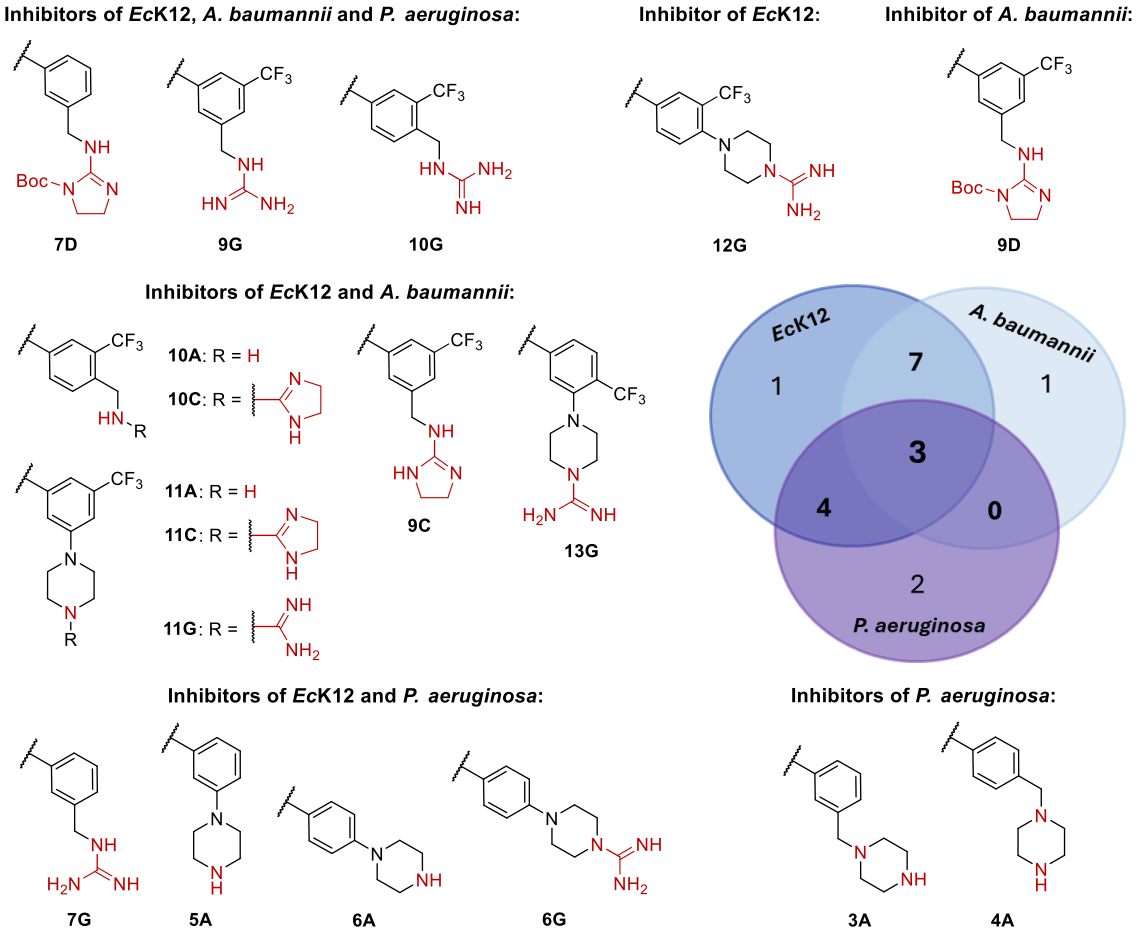

Figure 4. Chemical structures and Venn diagram of the active compounds in *Escherichia coli* K12 (*Ec*K12), *Acinetobacter baumannii, and Pseudomonas aeruginosa* (≥ 45% inhibition at 50 μM). Ionisable nitrogen moieties in red.

Gram-positive bacteria. The use of Hergenrother's eNTRy rules has been mostly reported by modifying a Gram-positive antibacterial class to comply with the three structural indications and thereby obtaining GNB activity. Therefore, we wanted to assess the GPB inhibition of our pyrazole-amide class and tested all 48 compounds against *S. aureus* and *S. pneumoniae*. Half of the compounds were active against at least one of the species but only one example of a neutral control compound (**9B**) inhibits *S. pneumoniae* (**9B**: MIC_{95} = 30 μM, Table 1). This finding suggests that the bacterial permeability of our neutral compounds is very low. However, our methodology was set up for the assessment of antibacterial activity of the chemical class, we did not quantify bioavailability of our compounds, therefore we cannot rule out that the ionisable nitrogen atoms are contributing significantly to the on-target activity. Eighteen of the 24 Gram-positive hits inhibit both *S. aureus* and *S. pneumoniae*, with potencies against *S. aureus* being generally higher and guanidines being particularly favourable. Guanidines **9**–**10C** and **9**–**13G** have excellent single digit micromolar MIC_{95} values against *S. aureus*. In addition, **11A** and **11C** are among the best hits in both

species and amine **12A** in *S. pneumoniae*. These findings align with previous trends and highlight the favourable combination of trifluoromethyl and positively charged motifs for antibacterial activity. In the case of *S. pneumoniae*, piperazine substituents are especially advantageous.

Mycobacterium tuberculosis. To obtain an even wider scope of the anti-infective profile of our chemical class, we assessed its antitubercular activity using the *M. tuberculosis* strain *Mtb*H37Rv and obtained 22 hits. The five best *Mtb*H37Rv inhibitors (**10**–**13G**, **11C**) have comparable potencies to the best Gram-positive and *Ec*Δ*tolC* hits, with an MIC_{90} value of 4 µM **12G** is the most potent *Mtb*H37Rv inhibitor (Table 1). The tendency of CF_3 and guanidine-containing structures to be especially active persists, and overall there is a big overlap in hit compounds shared between *Mtb*H37Rv, GPB and *Ec*Δ*tolC* (Figure 3). Our neutral control compounds were not sufficiently soluble in the *M. tuberculosis* growth medium and could not be evaluated (Table S2). Similarly, four amines had low solubilities (16–32 µM: **2**, **4A**, **6A**, **12A**) and did not show an effect on the growth of *Mtb*H37Rv at the testable concentrations (Table 1). To the best of our knowledge, this is the first record of applying the eNTRy rules to gain antitubercular activity, and was encouraged in a review on the hurdles of anti tubercular drug development from 2020.[37] However, similarly to the other tested pathogens, we cannot rule out that the ionisable nitrogen functionalities give rise to the antibacterial effect and not only to the bacterial uptake. Especially considering that the membrane of *M. tuberculosis is* particularly lipophilic and hard to permeate for drug-like compounds.[38]

Cytotoxicity. To get an insight into the toxicity of the class, the impact on the viability of the human liver cell line HepG2 was evaluated for all compounds. Generally, our most potent hits were nontoxic with cytotoxic concentrations (CC_{50}) >50 µM (Table 1). However, we did identify a major cytotoxic liability. All amine derivatives had a toxic effect on the liver cells, in the worst cases the CC_{50} values reached the single-digit micromolar range. Interestingly, the majority of Boc and guanidine analogues were not toxic, suggesting that the liability stems directly from the amine functional groups. This is exemplified when comparing the toxicities of structures **5**–**8**. Compounds **5** and **6** contain a piperazine-substituted phenyl, in *meta* and *para*. In the closely-related structures **7** and **8**, a methylene linker separates the piperazine from the aromatic ring, which results in both piperazine nitrogen atoms being aliphatic amines. In this case, both the amine (**7**–**8A**) and the Boc (**7**–**8B**) derivatives are toxic. In contrast, Boc and guanidine derivatives **5**–**6B** and **5**–**6G** are nontoxic, whereas amine analogues **5**–**6A** are, indicating that aniline-like nitrogen atoms devoid of hepatoxicity.

We investigated the toxicity of our best *Mtb*H37Rv inhibitors further by testing their effect on human monocyte-derived macrophages (**10**–**13G**, Table S2). None of the tested compounds were of major concern, solely **12G** exhibits a CC_{90} of 32 µM, which is manageable given that it is an eightfold difference in activity compared to *Mtb*H37Rv.

Conclusions

We report the design, synthesis, and evaluation of a small library of pyrazole-amides against *P. falciparum*, *E. coli, A. baumannii*, *P. aeruginosa*, *S. pneumoniae*, *S. aureus*, and *M. tuberculosis*. Through phenotypic screenings, we identified broad-spectrum anti-infective activity of the new pyrazole-amide class. We successfully applied the eNTRy rules to an antimalarial compound extending its activity not only to GNB but also GPB and *M. tuberculosis*. The best ionisable nitrogen-containing functional group for our chemical class were *N*-alkyl guanidines. For the first time, we showed that cyclised guanidines can also aid in bacterial uptake. We identified three compounds (**3D**, **9**–**10G**) with activity in all tested GNB. **12G** is the most potent *Mtb*H37Rv, *Ec*Δ*tolC* and *S. aureus* hit with low single-digit micromolar activities in all three species, while maintaining the antimalarial potency of the parent compound **1a**. We observed the biggest SAR variations in *P. aeruginosa*, where guanidines or trifluoromethyl substitution seemed detrimental to activity opposed to the rest of the pathogens. Further evaluation of molecular properties that dictate compounds' bioavailabilities across different pathogens is needed to better understand the applicability and limitations of existing guidelines and expand them. At the same time, the target identification of the pyrazole-amide class is necessary for future hit-optimisation and better rationalisation of the SAR.

Author Contributions

M. Braun-Cornejo was involved in designing the project, synthesising compounds, and writing of the manuscript. M. Platteschorre and V. de Vries were involved in synthesising compounds. P. Bravo performed and evaluated the *Pf*NF54 activity tests. V. Sonawane performed and evaluated the *Mtb*H37Rv activity tests. M. M. Hamed was involved in purification of compounds. J. Haupenthal coordinated and evaluated the bacterial and HepG2 activity tests. N. Reiling, M. Rottmann, and D. Piet were involved in supervising the project. P. Maas, E. Diamanti, and A.K. H. Hirsch were involved in designing and supervising the project. All authors edited or approved the submitted manuscript.

Acknowledgements

This project has received funding from the European Union's Horizon 2020 research and innovation programme under the Marie Skłodowska-Curie grant agreement No. 860816 (A. K. H. Hirsch, P. Maas, M. Rottmann, & N. Reiling). The authors thank Nanda de Klerk-Sprenkels for expert support in NMR.

Notes

The authors declare no competing financial interest.

References

(1) Murray, C. J.; Ikuta, K. S.; Sharara, F.; Swetschinski, L.; Robles Aguilar, G.; Gray, A.; Han, C.; Bisignano, C.; Rao, P.; Wool, E.; Johnson, S. C.; Browne, A. J.; Chipeta, M. G.; Fell, F.; Hackett, S.; Haines-Woodhouse, G.; Kashef Hamadani, B. H.; Kumaran, E. A. P.; McManigal, B.; Agarwal, R.; Akech, S.; Albertson, S.; Amuasi, J.; Andrews, J.; Aravkin, A.; Ashley, E.; Bailey, F.; Baker, S.; Basnyat, B.; Bekker, A.; Bender, R.; Bethou, A.; Bielicki, J.; Boonkasidecha, S.; Bukosia, J.; Carvalheiro, C.; Castañeda-Orjuela, C.; Chansamouth, V.; Chaurasia, S.; Chiurchiù, S.; Chowdhury, F.; Cook, A. J.; Cooper, B.; Cressey, T. R.; Criollo-Mora, E.; Cunningham, M.; Darboe, S.; Day, N. P. J.; De Luca, M.; Dokova, K.; Dramowski, A.; Dunachie, S. J.; Eckmanns, T.; Eibach, D.; Emami, A.; Feasey, N.; Fisher-Pearson, N.; Forrest, K.; Garrett, D.; Gastmeier, P.; Giref, A. Z.; Greer, R. C.; Gupta, V.; Haller, S.; Haselbeck, A.; Hay, S. I.; Holm, M.; Hopkins, S.; Iregbu, K. C.; Jacobs, J.; Jarovsky, D.; Javanmardi, F.; Khorana, M.; Kissoon, N.; Kobeissi, E.; Kostyanev, T.; Krapp, F.; Krumkamp, R.; Kumar, A.; Kyu, H. H.; Lim, C.; Limmathurotsakul, D.; Loftus, M. J.; Lunn, M.; Ma, J.; Mturi, N.; Munera-Huertas, T.; Musicha, P.; Mussi-Pinhata, M. M.; Nakamura, T.; Nanavati, R.; Nangia, S.; Newton, P.; Ngoun, C.; Novotney, A.; Nwakanma, D.; Obiero, C. W.; Olivas-Martinez, A.; Olliaro, P.; Ooko, E.; Ortiz-Brizuela, E.; Peleg, A. Y.; Perrone, C.; Plakkal, N.; Ponce-de-Leon, A.; Raad, M.; Ramdin, T.; Riddell, A.; Roberts, T.; Robotham, J. V.; Roca, A.; Rudd, K. E.; Russell, N.; Schnall, J.; Scott, J. A. G.; Shivamallappa, M.; Sifuentes-Osornio, J.; Steenkeste, N.; Stewardson, A. J.; Stoeva, T.; Tasak, N.; Thaiprakong, A.; Thwaites, G.; Turner, C.; Turner, P.; van Doorn, H. R.; Velaphi, S.; Vongpradith, A.; Vu, H.; Walsh, T.; Waner, S.; Wangrangsimakul, T.; Wozniak, T.; Zheng, P.; Sartorius, B.; Lopez, A. D.; Stergachis, A.; Moore, C.; Dolecek, C.; Naghavi, M. Global Burden of Bacterial Antimicrobial Resistance in 2019: A Systematic Analysis. *The Lancet* **2022**, *399* (10325), 629–655. https://doi.org/10.1016/S0140-6736(21)02724-0.

(2) World Health Organization. *Global Priority List of Antibiotic-Resistant Bacteria to Guide Research, Discovery, and Development of New Antibiotics - 2017*; Geneva, 2017.

(3) Walesch, S.; Birkelbach, J.; Jézéquel, G.; Haeckl, F. P. J.; Hegemann, J. D.; Hesterkamp, T.; Hirsch, A. K. H.; Hammann, P.; Müller, R. Fighting Antibiotic Resistance—Strategies and (Pre)Clinical Developments to Find New Antibacterials. *EMBO Rep* **2023**, *24* (1). https://doi.org/10.15252/embr.202256033.

(4) Lewis, K. The Science of Antibiotic Discovery. *Cell*. Cell Press April 2, 2020, pp 29–45. https://doi.org/10.1016/j.cell.2020.02.056.

(5) Pérez, A.; Poza, M.; Fernández, A.; Del Carmen Fernández, M.; Mallo, S.; Merino, M.; Rumbo-Feal, S.; Cabral, M. P.; Bou, G. Involvement of the AcrAB-TolC Efflux Pump in the Resistance, Fitness, and Virulence of Enterobacter Cloacae. *Antimicrob Agents Chemother* **2012**, *56* (4), 2084–2090. https://doi.org/10.1128/AAC.05509-11.

(6) Tamae, C.; Liu, A.; Kim, K.; Sitz, D.; Hong, J.; Becket, E.; Bui, A.; Solaimani, P.; Tran, K. P.; Yang, H.; Miller, J. H. Determination of Antibiotic Hypersensitivity among 4,000 Single-Gene-Knockout

Mutants of Escherichia Coli. *J Bacteriol* **2008**, *190* (17), 5981–5988. https://doi.org/10.1128/JB.01982-07.

(7) Sulavik, M. C.; Houseweart, C.; Cramer, C.; Jiwani, N.; Murgolo, N.; Greene, J.; Didomenico, B.; Shaw, K. J.; Miller, G. H.; Hare, R.; Shimer, G. Antibiotic Susceptibility Profiles of Escherichia Coli Strains Lacking Multidrug Efflux Pump Genes. *Antimicrob Agents Chemother* **2001**, *45* (4), 1126–1136. https://doi.org/10.1128/AAC.45.4.1126-1136.2001.

(8) Lien, E. J.; Hansch, C.; Anderson, S. M. Structure-Activity Correlations for Antibacterial Agents on Gram-Positive and Gram-Negative Cells. *J Med Chem* **1968**, *11* (3), 430–441. https://doi.org/10.1021/JM00309A004/ASSET/JM00309A004.FP.PNG_V03.

(9) Ropponen, H. K.; Richter, R.; Hirsch, A. K. H.; Lehr, C. M. Mastering the Gram-Negative Bacterial Barrier – Chemical Approaches to Increase Bacterial Bioavailability of Antibiotics. *Advanced Drug Delivery Reviews*. Elsevier B.V. May 1, 2021, pp 339–360. https://doi.org/10.1016/j.addr.2021.02.014.

(10) Richter, M. F.; Drown, B. S.; Riley, A. P.; Garcia, A.; Shirai, T.; Svec, R. L.; Hergenrother, P. J. Predictive Compound Accumulation Rules Yield a Broad-Spectrum Antibiotic. *Nature 2017 545:7654* **2017**, *545* (7654), 299–304. https://doi.org/10.1038/nature22308.

(11) Richter, M. F.; Hergenrother, P. J. The Challenge of Converting Gram-Positive-Only Compounds into Broad-Spectrum Antibiotics. *Ann N Y Acad Sci* **2019**, *1435* (1), 18–38. https://doi.org/10.1111/nyas.13598.

(12) Smith, P. A.; Koehler, M. F. T.; Girgis, H. S.; Yan, D.; Chen, Y.; Chen, Y.; Crawford, J. J.; Durk, M. R.; Higuchi, R. I.; Kang, J.; Murray, J.; Paraselli, P.; Park, S.; Phung, W.; Quinn, J. G.; Roberts, T. C.; Rougé, L.; Schwarz, J. B.; Skippington, E.; Wai, J.; Xu, M.; Yu, Z.; Zhang, H.; Tan, M.-W.; Heise, C. E. Optimized Arylomycins Are a New Class of Gram-Negative Antibiotics. *Nature* **2018**, *561* (7722), 189–194. https://doi.org/10.1038/s41586-018-0483-6.

(13) Hu, Y.; Shi, H.; Zhou, M.; Ren, Q.; Zhu, W.; Zhang, W.; Zhang, Z.; Zhou, C.; Liu, Y.; Ding, X.; Shen, H. C.; Yan, S. F.; Dey, F.; Wu, W.; Zhai, G.; Zhou, Z.; Xu, Z.; Ji, Y.; Lv, H.; Jiang, T.; Wang, W.; Xu, Y.; Vercruysse, M.; Yao, X.; Mao, Y.; Yu, X.; Bradley, K.; Tan, X. Discovery of Pyrido[2,3- b]Indole Derivatives with Gram-Negative Activity Targeting Both DNA Gyrase and Topoisomerase IV. *J Med Chem* **2020**, *63* (17), 9623–9649. https://doi.org/10.1021/acs.jmedchem.0c00768.

(14) Liu, B.; Trout, R. E. L.; Chu, G. H.; Mcgarry, D.; Jackson, R. W.; Hamrick, J. C.; Daigle, D. M.; Cusick, S. M.; Pozzi, C.; De Luca, F.; Benvenuti, M.; Mangani, S.; Docquier, J. D.; Weiss, W. J.; Pevear, D. C.; Xerri, L.; Burns, C. J. Discovery of Taniborbactam (VNRX-5133): A Broad-Spectrum Serine- And Metallo-β-Lactamase Inhibitor for Carbapenem-Resistant Bacterial Infections. *J Med Chem* **2020**, *63* (6), 2789–2801. https://doi.org/10.1021/acs.jmedchem.9b01518.

(15) Schumacher, C. E.; Rausch, M.; Greven, T.; Neudörfl, J. M.; Schneider, T.; Schmalz, H. G. Total Synthesis and Antibiotic Properties of Amino-Functionalized Aromatic Terpenoids Related to Erogorgiaene and the Pseudopterosins. *European J Org Chem* **2022**, *2022* (26). https://doi.org/10.1002/ejoc.202200058.

(16) Parker, E. N.; Cain, B. N.; Hajian, B.; Ulrich, R. J.; Geddes, E. J.; Barkho, S.; Lee, H. Y.; Williams, J. D.; Raynor, M.; Caridha, D.; Zaino, A.; Shekhar, M.; Muñoz, K. A.; Rzasa, K. M.; Temple, E. R.; Hunt, D.; Jin, X.; Vuong, C.; Pannone, K.; Kelly, A. M.; Mulligan, M. P.; Lee, K. K.; Lau, G. W.; Hung, D. T.; Hergenrother, P. J. An Iterative Approach Guides Discovery of the FabI Inhibitor Fabimycin, a Late-Stage Antibiotic Candidate with In Vivo Efficacy against Drug-Resistant Gram-Negative Infections. *ACS Cent Sci* **2022**, *8* (8), 1145–1158. https://doi.org/10.1021/acscentsci.2c00598.

(17) Motika, S. E.; Ulrich, R. J.; Geddes, E. J.; Lee, H. Y.; Lau, G. W.; Hergenrother, P. J. Gram-Negative Antibiotic Active through Inhibition of an Essential Riboswitch. *J Am Chem Soc* **2020**, *142* (24), 10856–10862. https://doi.org/10.1021/jacs.0c04427.

(18) Fortney, K. R.; Smith, S. N.; van Rensburg, J. J.; Brothwell, J. A.; Gardner, J. J.; Katz, B. P.; Ahsan, N.; Duerfeldt, A. S.; Mobley, H. L. T.; Spinola, S. M. CpxA Phosphatase Inhibitor Activates CpxRA and Is a Potential Treatment for Uropathogenic Escherichia Coli in a Murine Model of Infection. *Microbiol Spectr* **2022**, *10* (2). https://doi.org/10.1128/spectrum.02430-21.

(19) Perlmutter, S. J.; Geddes, E. J.; Drown, B. S.; Motika, S. E.; Lee, M. R.; Hergenrother, P. J. Compound Uptake into *E. Coli* Can Be Facilitated by *N* -Alkyl Guanidiniums and Pyridiniums. *ACS Infect Dis* **2021**, *7* (1), 162–173. https://doi.org/10.1021/acsinfecdis.0c00715.

(20) Masci, D.; Hind, C.; Islam, M. K.; Toscani, A.; Clifford, M.; Coluccia, A.; Conforti, I.; Touitou, M.; Memdouh, S.; Wei, X.; La Regina, G.; Silvestri, R.; Sutton, J. M.; Castagnolo, D. Switching on the Activity of 1,5-Diaryl-Pyrrole Derivatives against Drug-Resistant ESKAPE Bacteria: Structure-Activity Relationships and Mode of Action Studies. *Eur J Med Chem* **2019**, *178*, 500–514. https://doi.org/10.1016/j.ejmech.2019.05.087.

(21) Stoorza, A. M.; Duerfeldt, A. S. Guiding the Way: Traditional Medicinal Chemistry Inspiration for Rational Gram-Negative Drug Design. *Journal of Medicinal Chemistry*. American Chemical Society January 11, 2024, pp 65–80. https://doi.org/10.1021/acs.jmedchem.3c01831.

(22) Zgurskaya, H. I.; López, C. A.; Gnanakaran, S. Permeability Barrier of Gram-Negative Cell Envelopes and Approaches to Bypass It. *ACS Infect Dis* **2016**, *1* (11), 512–522. https://doi.org/10.1021/acsinfecdis.5b00097.

(23) Sohlenkamp, C.; Geiger, O. Bacterial Membrane Lipids: Diversity in Structures and Pathways. *FEMS Microbiol Rev* **2016**, *40* (1), 133–159. https://doi.org/10.1093/femsre/fuv008.

(24) Andrews, L. D.; Kane, T. R.; Dozzo, P.; Haglund, C. M.; Hilderbrandt, D. J.; Linsell, M. S.; Machajewski, T.; McEnroe, G.; Serio, A. W.; Wlasichuk, K. B.; Neau, D. B.; Pakhomova, S.; Waldrop, G. L.; Sharp, M.; Pogliano, J.; Cirz, R. T.; Cohen, F. Optimization and Mechanistic Characterization of Pyridopyrimidine Inhibitors of Bacterial Biotin Carboxylase. *J Med Chem* **2019**, *62* (16), 7489–7505. https://doi.org/10.1021/acs.jmedchem.9b00625.

(25) Hu, Z.; Leus, I. V.; Chandar, B.; Sherborne, B. S.; Avila, Q. P.; Rybenkov, V. V.; Zgurskaya, H. I.; Duerfeldt, A. S. Structure-Uptake Relationship Studies of Oxazolidinones in Gram-Negative ESKAPE Pathogens. *J Med Chem* **2022**, *65* (20), 14144–14179. https://doi.org/10.1021/acs.jmedchem.2c01349.

(26) Ropponen, H.; Diamanti, E.; Johannsen, S.; Illarionov, B.; Hamid, R.; Jaki, M.; Sass, P.; Fischer, M. Exploring the Translational Gap of a Novel Class of Escherichia Coli IspE Inhibitors. *ChemMedChem* **2023**, *e202300346* (18). https://doi.org/10.1002/cmdc.202300346.

(27) Ropponen, H. K.; Diamanti, E.; Siemens, A.; Illarionov, B.; Haupenthal, J.; Fischer, M.; Rottmann, M.; Witschel, M.; Hirsch, A. K. H. Assessment of the Rules Related to Gaining Activity against Gram-Negative Bacteria. *RSC Med Chem* **2021**, *12* (4), 593–601. https://doi.org/10.1039/d0md00409j.

(28) Gaspar, A.; Reis, J.; Matos, M. J.; Uriarte, E.; Borges, F. In Search for New Chemical Entities as Adenosine Receptor Ligands: Development of Agents Based on Benzo-γ-Pyrone Skeleton. *Eur J Med Chem* **2012**, *54*, 914–918. https://doi.org/10.1016/j.ejmech.2012.05.033.

(29) Santos, C. M. M.; Silva, V. L. M.; Silva, A. M. S. Synthesis of Chromone-Related Pyrazole Compounds. *Molecules* **2017**, *22* (10). https://doi.org/10.3390/molecules22101665.

(30) Rodríguez-Soacha, D. A.; Fender, J.; Ramírez, Y. A.; Collado, J. A.; Muñoz, E.; Maitra, R.; Sotriffer, C.; Lorenz, K.; Decker, M. “Photo-Rimonabant”: Synthesis and Biological Evaluation of Novel Photoswitchable Molecules Derived from Rimonabant Lead to a Highly Selective and Nanomolar “ *Cis* -On” CB $_1$ R Antagonist. *ACS Chem Neurosci* **2021**, *12* (9), 1632–1647. https://doi.org/10.1021/acschemneuro.1c00086.

(31) Hermann, T.; Hochegger, P.; Dolensky, J.; Seebacher, W.; Pferschy-Wenzig, E.-M.; Saf, R.; Kaiser, M.; Mäser, P.; Weis, R. Synthesis and Structure-Activity Relationships of New 2-Phenoxybenzamides with Antiplasmodial Activity. *Pharmaceuticals* **2021**, *14* (11), 1109. https://doi.org/10.3390/ph14111109.

(32) Chen, D.; Sun, X.; Shan, Y.; You, J. One-Pot Synthesis of Polyfunctionalized Quinolines *via* a Copper-Catalyzed Tandem Cyclization. *Org Biomol Chem* **2018**, *16* (41), 7657–7662. https://doi.org/10.1039/C8OB02078G.

(33) Svenningsen, S. W.; Frederiksen, R. F.; Counil, C.; Ficker, M.; Leisner, J. J.; Christensen, J. B. Synthesis and Antimicrobial Properties of a Ciprofloxacin and PAMAM-Dendrimer Conjugate. *Molecules* **2020**, *25* (6). https://doi.org/10.3390/molecules25061389.

(34) Dardonville, C.; Caine, B. A.; Navarro De La Fuente, M.; Martín Herranz, G.; Corrales Mariblanca, B.; Popelier, P. L. A. Substituent Effects on the Basicity (p: K a) of Aryl Guanidines and 2-(Arylimino)Imidazolidines: Correlations of PH-Metric and UV-Metric Values with Predictions from Gas-Phase Ab Initio Bond Lengths. *New Journal of Chemistry* **2017**, *41* (19), 11016–11028. https://doi.org/10.1039/c7nj02497e.

(35) Ueno, H.; Yokota, K.; Hoshi, J. I.; Yasue, K.; Hayashi, M.; Hase, Y.; Uchida, I.; Aisaka, K.; Katoh, S.; Cho, H. Synthesis and Structure-Activity Relationships of Novel Selective Factor Xa Inhibitors with a Tetrahydroisoquinoline Ring. *J Med Chem* **2005**, *48* (10), 3586–3604. https://doi.org/10.1021/jm058160e.

(36) Aoyagi, N.; Endo, T. Synthesis of Five- and Six-Membered Cyclic Guanidines by Guanylation with Isothiouronium Iodides and Amines under Mild Conditions. *Synth Commun* **2017**, *47* (5), 442–448. https://doi.org/10.1080/00397911.2016.1269927.

(37) Dalberto, P. F.; de Souza, E. V.; Abbadi, B. L.; Neves, C. E.; Rambo, R. S.; Ramos, A. S.; Macchi, F. S.; Machado, P.; Bizarro, C. V.; Basso, L. A. Handling the Hurdles on the Way to Anti-Tuberculosis Drug Development. *Front. Chem.* **2020**, *8* (586294). https://doi.org/10.3389/fchem.2020.586294.

(38) Batt, S. M.; Minnikin, D. E.; Besra, G. S. The Thick Waxy Coat of Mycobacteria, a Protective Layer against Antibiotics and the Host's Immune System. *Biochemical Journal* **2020**, *477* (10), 1983–2006. https://doi.org/10.1042/BCJ20200194.